A Muscle-Reflex Model of Forelimb and Hindlimb of Felidae Family of Animal with Dynamic Pattern Formation Stimuli

Azhar Aulia Saputra
Graduate School of Systems Design
Tokyo Metropolitan University
Tokyo, Japan
azhar-aulia-saputra@ed.tmu.ac.jp

Chin Wei Hong
Graduate School of Systems Design
Tokyo Metropolitan University
Tokyo, Japan
weihong@tmu.ac.jp

Auke Jan Ijspeert
Biorobotics Laboratory
Ecole Polytechnique Federale de Lausanne
Lausanne, Switzerland
auke.ijspeert@epfl.ch

Naoyuki Kubota
Graduate School of Systems Design
Tokyo Metropolitan University
Tokyo, Japan
kubota@tmu.ac.jp

***Abstract*—Human and animal locomotion are controlled by complex neural circuits, which can also serve as inspiration for designing locomotion controllers for dynamic locomotion in legged robots. We develop a locomotion controller model including a central pattern generator (CPGs) and a muscle reflex based on the forelimb and hindlimb structures of a cat. In this paper, we focus on modeling the muscle reflex and its optimization. This muscle reflex model regulates ground force afferents in each limb. There are two phases in each step performed by this model, the swing and stance phases. The muscle during swing phase is activated by a pattern formation signal from the CPG. During stance phase, the muscle is automatically controlled by the moving speed. We utilize a multi-objective evolutionary algorithm to optimize parameters of the model. We use the proposed model to control a cat-like robot in simulations using Open Dynamics Engine. Results show that the simulated robot is able to move at different speeds by modulating simple stimulation signals to the CPG without needing to modify muscle and reflex parameters.**

***Index Terms*—Muscle reflex model, Bio-mimetic robot locomotion, Multi-objectives Optimization**

I. Introduction

Researchers are pursuing the design of human-like and animal-like robots because of its advantages. Some researchers have developed robots focusing on communication and social skills. Nonetheless, it is also essential to develop locomotion as support to robots movements. Conventional method [1], [2] with bottom-up model using planning-based development is popular to realize robot locomotion. Researchers also considered interdisciplinary viewpoints, such as biological approach, in their works of robot locomotion. Bio-inspired models with central pattern generation (CPG) locomotion have been proposed previously [3], [4] for legged robot implementation. Some researchers implemented muscle model as target actuator for mimicking human or animal locomotion [5]. However, existing models have yet to achieve dynamic locomotion as human or animal does. In this paper, we proposed the locomotion model for the quadruped robot by taking the benefit of the biological model in quadruped animals.

Locomotion principles have been proposed in terms of limbed element. However, it is unclear how this principle works to regulate motor control in human or animal. Therefore, analyzing natural integration is important to find the role of motor control. Human or animal involves a complex architecture of the neurons to produce their locomotion. Basically, locomotion pattern is produced by CPG in spinal cord interconnected by other motor neural pools to stimulate and synchronize with muscle synergies [6], [7], [8]. This spinal reflex has a big contribution in movement pattern control, muscle stimulation, and CPG modulation. Quadruped animal can demonstrate that CPG produces variations in gait patterns such as walking, trotting, running, and galloping [9]. Spinal reflexes will incorporate mechanical sensory information by alpha motoneurons bypassing central inputs into muscle activation.

Researchers have developed muscle-based model for both biped and quadruped robots. They focused on the development of mechanical design based on the musculoskeletal model. Some researchers developed musculoskeletal based actuator for their quadruped robot. They also succeeded developing its stable locomotion [10], [11]. Other researchers focused on locomotion control using musculoskeletal model. Toeda et al, have designed the locomotion model of rats based on the CPG and the muscle model [12]. However, the model is still far to be applied to robotics implementation. Besides, the development of both forelimb and hindlimb muscle reflex model is still few. In this paper, our contribution is development of a muscle-based locomotion model inspired by cat musculoskeletal model. We are exploring further the benefit of locomotion process in biological system for its application in dynamic locomotion of legged robotics. It shows not only the

978-1-7281-6926-2/20/$31.00 ©2020 IEEE

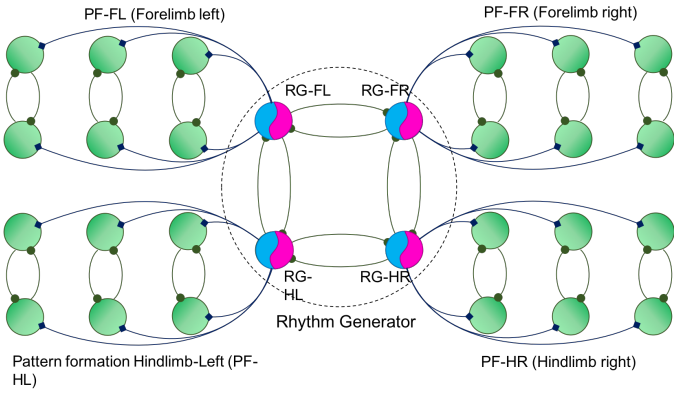

Figure 1. Design of two layered CPG with distributed rhythm generator and pattern formation

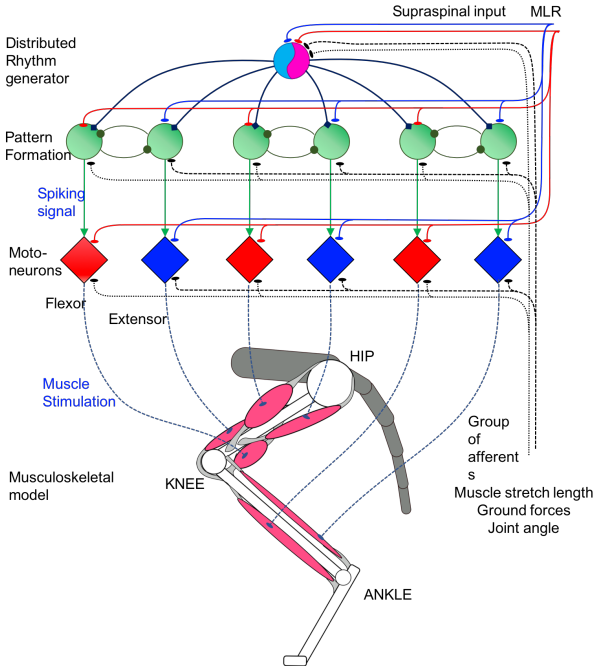

Figure 2. Design of integration between cpg and muscle model

locomotion performance in robotics but also the mechanism of locomotion process in a cat.

This paper is organized as follows. Section II shows the multi-layer CPG model for controlling the muscle activation pattern. After that, we explain the cat-like hindlimb and forelimb muscle model used in the proposed model in Section III. In order to prove the reliability of the proposed model, we show several appropriate experiments in Section IV. Finally, we conclude and discuss further development.

II. Integrated CPG Model

CPG model reflects neural circuit in spinal cord, which can produce primary rhythmic locomotive signal. The signal still can be produced even when there is no supraspinal level driven signal [7]. Our designed CPG model is based on the study of locomotion model mechanism in human and animal. We modified the model of a single generator based CPG proposed in [8], [13] into two-layered model CPG. Our modified CPG consists of distributed single rhythm generator (RG) and model of pattern formation (PF). One RG neuron represents one leg and one PF neuron represents one muscle. The proposed CPG model can be seen in Fig. 1.

A. Rhythm generator

RG neurons in one leg generate rhythmic signal to PF neurons in the same leg. RG neuron generates dynamic rhythmic pattern by synchronizing with sensory feedback. The rhythmic pattern can be generated in the absence of any sensory information from the receptor skin, joints, and muscle [14], [15]. The inner state of RG neuron is based on the neural oscillator proposed by Matsuoka that shows reciprocal inhibition effect [16], [17]. The rhythm generator used has similar model with our previous model proposed in [18], [19].

B. Pattern formation model

Signal generated by RG neurons will be transmitted to connected PF neurons. The purpose of PF neuron pools is to control activation time of each muscle stimulation in when the leg starts swinging. The PF neurons will generate a firing signal to activate the muscle when the leg starts to swing. In this model, we utilize modified spiking neural network in order for PF neuron to generate firing signal. The PF neuron in ith joint (PF_i) calculated as

$$PF_{i,k}(t) = e^{\left(\log(0.5)\times\left(\frac{|pf_i-\mu|}{(\mu\times w)}^3\right)\right)} \quad (1)$$

$$pf_i(t) = pf_i(t-1) + p_i \quad (2)$$

where μ represents the starting control calculated by $\mu = (30-\phi_i^{(LEG)})/30$, w represents the time of activation signal calculated as $w = \psi_i^{(LEG}/50$. $\phi_i^{(LEG)}$ and $\psi_i^{(LEG}$ are the parameter for controlling swing activation and timing of ith PF neuron in certain LEG, F for forelimb and H for hindlimb. The value of ϕ and ψ will be optimized in using multi-objective evolutionary algorithm. p_i is the spike signal generated from:

$$p_i = \begin{cases} 1 & \text{if } h_i \geq \Theta \\ 0 & \text{otherwise} \end{cases} \quad (3)$$

When internal state of PF neurons h_i is higher than a threshold for firing Θ), then the spike value becomes 1. Inner state of the i-th neuron (h_i) is calculated as follow:

$$h_i(t) = tanh\left(h_i^{syn}(t) + h_i^{ext}(t) + h_i^{ref}(t)\right) \quad (4)$$

where, $h_i^{syn}(t)$ includes the weighted pulse outputs from other neurons and the reduced value of internal state in the previous timestep calculated as:

$$h_i^{syn}(t) = \gamma^{syn}\cdot h_j^{(PSP)}(t) + \sum_{j=1,j\neq i}^{N} \mathbf{w}_{ij}(t+1)h_j^{(PSP)}(t) \quad (5)$$

where γ^{syn} is the temporal discount rate of h_i, w_{ij} is a weight from the i-th PF neuron to the j-th PF neuron. Then $h_j^{PSP}(t)$

is the Post Synaptic Potential (PSP) approximately transmit calculated as

$$h_i^{PSP}(t) = exp\Big(-(t - t_i^{((f))})/\tau_i \Big) \tag{6}$$

where $t_i^{(f)}$ is the last firing of the neuron i, and τ_i is a parameter which influences how long the firing of the neuron has an effect to the connecting neurons. $h_i^{ref}(t)$ will be calculated as:

$$h_i^{ref}(t) = \begin{cases} \gamma^{ref} \cdot h_i^{ref}(t-1) - R & \text{if } p_i(t-1) = 1 \\ \gamma^{ref} \cdot h_i^{ref}(t-1) & \text{otherwise} \end{cases} \tag{7}$$

$h_i^{ref}(t)$ is used for representing the refractories of the neuron. This means that after the neuron fired, its internal state value decreased using the refractories component, in order to avoid the continuous firing of the neuron within a short time. The value of R will be subtracted after the p_i is fired. $R > 0$, γ^{ref} is a discount rate of h_i^{ref}, and $0 \leq \gamma^{ref} \leq 1 \cdot P_i(t)$ will be generated to muscle model as activation input. $h_i^{ext}(t)$ is the pattern signal input to the *i*-th neuron generated from central pattern generator.

The value from PF_i will be transmitted to the muscle model to generate swing behavior.

III. Musculoskeletal Model

We design the reflex model of hindlimb and forelimb based on mammal structure. Human beings have only hindlimb to support their body for locomotion. However, most legged mammals use both hindlimb and forelimb to support their locomotion [20]. Some researchers have proposed the stance and swing phase in muscle integrated locomotion. Extensor muscle is involved in stance phase and flexor muscle is involved in swing phase.

The investigation process of stance-swing phase transition have shown that transition is controlled by sensory signals from leg proprioceptors. Some of the receptors providing these signals have been identified [14].

Stepping are process involving swing and stance transition inseparably [21], [22]. Swing to stance phase transition should be activated automatically based on stimuli from ground force and hip position. Thus, swing to stance transition is the best timing for controlling movement pattern. We control the swing stimulation by signal pattern modulation generated by neural oscillator proposed by Matsuoka. One CPG neuron represents one joint. This signal will stimulate muscle reflex to perform swing phase. The proposed method consists of hindlimb and forelimb control model as shown in Figure 3.

A. Hindlimb reflex model

We are referring to the rhythmic motion study of the cat, where proximal and distal leg segments retain their relative angular orientation for most parts of the cyclic motion. Compliance mechanism is implemented between ankle and knee joint [23], [24]. We implement some important muscles and chose two muscle in one joint: 1) iliopsoas (IP, hip flexor) 2) Bicep femoris anterior (BFA, hip extensor) 3) biceps femoris posterior (BFP, knee flexor, and hip extensor) 4) Vastii (VA,

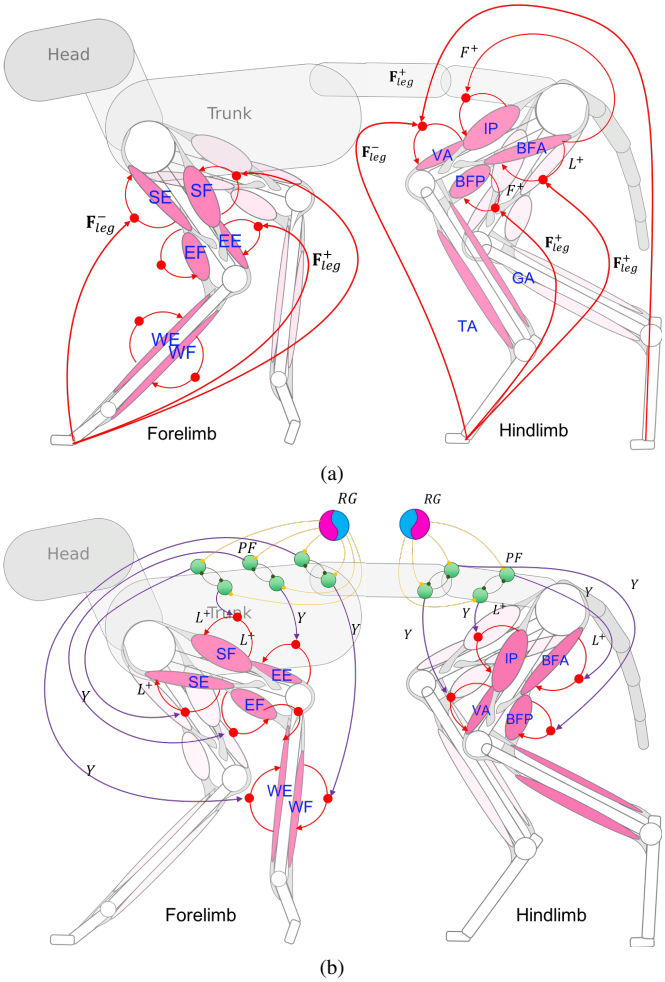

Figure 3. The muscle reflex structure during its phase. a) Muscle reflex structure in stance phase. b) Muscle reflex structure in swing phase.

knee extensor). We build the force reflex from the same leg (F_{leg}) and from the other 3 legs (F_{leg}^A, F_{leg}^B, F_{leg}^C), where A, B, C, are the contralateral hindlimb, ipsilateral forelimb, and contralateral forelimb, respectively.

1) Stance phase of hindlimb reflex model: During the stance phase, the muscle stimulation mostly effected by the ground reaction force (F_{leg}^A) [25], [26]. The ground force signal stimulates positive feedback to extensor muscle in hip joint (BFA). BFA stimulation (S_{BFA}) gets force feedback from local leg (F_{leg}) with calculated in Eq (8). Where $l_{(CE,BFA)}$ is BFA fiber length and $l_{(off,BFA)}$ is its desired length offset. The BFA's stretch reflex prevents large extension torque in hip joint. To reduce inhibition effect to BFA, negative force feedback of BFA is given to hip flexor (IP). For representing the spring mechanism during the stance phase, VA is stimulated with its own muscle activity using F+. Then, to initiate the transition to swing phase, VA and BFP receive positive and negative feedback respectively from contralateral ground force feedback. The overall muscle stimulation for hindlimb during stance phase can be seen in the following equations:

$$S_{BFA}(t) = S_{0,BFA} + G^{F}_{BFA}F_{leg} \cdot G^{l}_{BFA}\left(l_{CE,BFA} - l_{off,BFA}\right) \quad (8)$$

$$S_{IP}(t) = S_{0,IP} + G^{f}_{IP}F_{leg} \cdot G^{l}_{IP}\left(l_{CE,IP} - l_{off,BFA}\right) \quad (9)$$

$$S_{BFP}(t) = S_{0,BFP} + C^{st}_{BFP} - G^{F}_{BFP}F^{A}_{leg}F^{B}_{leg} \quad (10)$$

$$S_{VA}(t) = S_{0,VA} + G^{F}_{VA}F^{A}_{leg}F^{B}_{leg} \quad (11)$$

2) Swing phase of hindlimb reflex model: The swing transition is initiated in the late stance phase, however, the swing movement is controlled and triggered by a signal from CPG. The ith CPG signal Y_i from neuron will trigger hip flexor muscle (IP) and knee flexor muscle (BFP) for several millisecond. To inhibit early extending process, IP receives stretch length reflex. Opposite muscle (BFA) also receives its stretch reflex to force the leg touching the ground. In the end of swing phase, extensor muscle of knee (VA) is stimulated after ending stimulation of CPG. At this time, BFP tends to be silent. The overall muscle stimulation for hindlimb during swing phase can be seen in the following equations:

$$S_{BFA}(t) = S_{0,BFA} - G^{y}_{BFA}Y_{IP} + G^{l,S}_{BFA}\left(l_{CE,BFA} - l_{off,BFA}\right) \quad (12)$$

$$S_{IP}(t) = S_{0,IP} + G^{y}_{IP}Y_{IP} + G^{l,S}_{IP}(l_{CE,IP} - l_{off,IP}) \quad (13)$$

$$S_{VA}(t) = S_{0,VA} - G^{Y}_{VA}Y_{IP} + C_{VA} \quad (14)$$

$$S_{BFP}(t) = S_{0,BFP} + G^{Y}_{BFP}Y_{BFP} - C_{BFP} + G^{F}_{BFP}F_{leg} \quad (15)$$

B. Forelimb reflex model

The forelimb has an important role as the stability controllerinstead of the locomotion. Forelimb tends to monitor stability and positioning rather than locomotion. Therefore it has greater action than hindlimb. Within forelimb, there are some neurological and physiological studies and observational work about muscle activity. Some research investigated the synchronization of muscle patterns in cat's forelimb motion [27], [28], [29].

Forelimb's movement is produced by many combined muscles, monoarticular and biarticular muscle[30]. In order to minimize the number of muscle without eliminating its characteristics, we cluster muscles in every joint into two groups: flexor and extensor muscle. In shoulder joint, we consider anterior deltoid, pectoralis major, and coracobrachialis muscle as flexor muscle, then latissimus dorsi, teres major and minor and posterior deltoid muscles as extensor muscle. There are two muscles in the shoulder and two muscles in the elbow joint (triceps (Tm) and brachialis (Br)). Then there are two muscles in the wrist (flexor carpi ulnaris and Palmaris Lungus for flexor, extensor Carpi Ulnaris and extensor Digitorum for extensor muscle). We only consider the monoarticular muscle in flexor or extensor action.

1) Stance phase of forelimb reflex model: In stance phase, extensor muscle of elbow, extensor muscle of wrist, and flexor muscle in the shoulder have stance-related activity predominantly. Shoulder flexor muscle activity starts 20-30 ms before forelimb lift-off, and continues until the end of the flexion epoch or slightly into E1. In elbow muscle, activity patterns of all extensors are similar in terms of onset and duration. All begin activity during E1, usually, after the onset of elbow extension, continue activity across limb placement, and cease activity just prior to limb lift-off. Activity in all flexors of elbow is also similar. In wrist joint, flexor muscle is activated in a similar phase with extensor muscle of elbow. After that, it will stop just prior to lift-off. The overall muscle stimulation for forelimb during stance phase can be seen in the following equations:

$$S_{SF}(t) = S_{0,SF} + G^{F}_{SF}F_{leg}G^{l}_{SF}(l_{CE,SF} - l_{off,SF}) + G^{F,A}_{SF}F^{A}_{leg} \quad (16)$$

$$S_{SE}(t) = S_{0,SE} - G^{F}_{SE}F^{A}_{leg}G^{l}_{SE}(l_{CE,SF} - l_{off,SF}) \quad (17)$$

$$S_{EE}(t) = S_{0,SE} + G^{F}_{SF}F^{A}_{leg} + C_{EE} \quad (18)$$

$$S_{EF}(t) = S_{0,EF} \quad (19)$$

$$S_{WE}(t) = S_{0,WE} + G^{F}_{WF}F^{A}_{leg} \quad (20)$$

$$S_{WF}(t) = S_{0,WF} + C_{WF} \quad (21)$$

2) Swing phase of forelimb reflex model: In swing phase, extensor muscle in shoulder joint is monophasically active during extension epoch. It begins activity during E1, and stop just before lift-off. Flexor muscle in elbow joint generally begins just prior to limb lift-off (F onset) and ceases at or near the onset of E1. Br, which is the only single joint flexor muscle of elbow, is active just prior to foot lift and remains active until approximately midswing. Cleidobrachialis (ClB) and biceps brachii (Bit) normally commence their periods of locomotor activity at about the same time as Br. The activity in ClB, however, always continue throughout the period of swing. Muscle related to wrist joint generally has low activity during swing phase [31]. In elbow muscle, activity patterns of all extensors are similar in terms of onset and duration. All begin activity during E1, usually, after onset of elbow extension, continue activity across limb placement, and cease activity just prior to limb lift-off. Activity in all flexors of elbow is also similar. In swing phase, flexor muscle in elbow joint generally begins just prior to limb lift-off (F onset) and ceases at or near the onset of E1. Br, which is the only single joint flexor muscle of elbow, is active just prior to foot lift and remains active until approximately midswing. Cleidobrachialis (ClB) and biceps brachii (Bit) normally commence their periods of locomotor activity at about the same time as Br. The activity in ClB, however, always continue throughout the period of swing. The overall muscle stimulation for forelimb during swing phase can be seen in the following equations:

$$S_{SF}(t) = S_{(0,SF} + G^{Y}_{SF}Y_{SF} + G^{l}_{SF}(l_{CE,SF} - l_{off,SF}) \quad (22)$$

$$S_{SE}(t) = S_{0,SE} - G^{Y}_{SE} Y_{SE} + G^{l}_{SE}(l_{CE,SF} - l_{off,SF}) \quad (23)$$

$$S_{EE}(t) = S_{0,SE} - G^{Y}_{EE} Y_{EE} + G^{l}_{EE} \cdot Y_{EE} \cdot (l_{EE} - (-l_{off,EF}) \quad (24)$$

$$S_{EF}(t) = S_{0,EF} - G^{Y}_{EF}(1 - Y_{EF}) + G^{l}_{EF} \cdot Y_{EF} \cdot (l_{EF} - l_{off,EF}) \quad (25)$$

$$S_{WE}(t) = S_{0,WE} + G^{Y}_{WE} Y_{WE} \quad (26)$$

$$S_{WF}(t) = S_{0,WF} + G^{Y}_{WF}(1 - Y_{WF}) \quad (27)$$

Detail explanation of the parameters can be seen in Table. I.

IV. Experimental result

In order to implement the proposed model, we built the cat-like robot simulation using the Open Dynamics Engine with its musculoskeletal model. We defined the intervals of the parameters empirically to specify the parameter search space for the optimization process. The parameter ranges can be seen in Table I. Furthermore, synaptic weights in CPG model and muscle reflex parameters are required to be optimized for generating appropriate signal pattern and activation signal. We optimized the parameters by using a multi-objective evolutionary algorithm (NSGA) where its fitness functions are calculated below in Eqs. (28) and (29)

$$F_1 = \begin{cases} f_{STIM} + f_{FALL} + 2 \cdot 10^4 \cdot (1.2 - f_{DIS}) & \text{if } f_{DIS \leq 1.2} \\ f_{STIM} + f_{FALL} & \text{otherwise} \end{cases} \quad (28)$$

$$F_2 = \begin{cases} f_{OSC}(1 + t_{STOP}/t_{MAX}) + 10 & \text{if } f_{DIS \leq 1.2} \\ f_{OSC}(1 + t_{STOP}/t_{MAX}) & \text{otherwise} \end{cases} \quad (29)$$

In the first fitness function (F_1), we consider the total muscle stimulation (f_{STIM}), falling condition (f_{FALL}), distance travelled (f_{DIS}), and movement oscillation (f_{OSC}). f_{STIM} calculated as follow:

$$f_{STIM} = \sum_{t=1}^{t_{MAX}} \sum_{n=1}^{N_{leg}} \sum_{m=1}^{N_m} S_m^{(leg)}(t) \quad (30)$$

where, N_m is the number of muscle in one leg and $S_m^{(n)}(t)$ is the stimulation of mth muscle in nth leg. Then, f_{FALL} parameter is calculated as follow:

$$f_{FALL} = 20 * (t_{MAX} - t_{STOP}) \quad (31)$$

t_{STOP} is the time when the robot fall down or the robot stop in the end of the performance ($t_{STOP} = t_{MAX}$). f_{DIS} is calculated as follow:

$$f_{DIS} = \sqrt{(d_l - l_{total})^2} \quad (32)$$

Where, d_l is the desired distance and l_{total} is the distance travelled. We set the value of d_l as 3. Furthermore, the movement oscillation f_{OSC} is calculated in below:

$$f_{OSC} = \sum_{t=1}^{T} \ddot{x}(t) \quad (33)$$

where, x(t) is the distance travelled in time t.

There are 32 parameters to be optimized using MOEA. Eight parameters are from pattern formation neurons and other 24 parameters are from muscle reflex model. We set the number of individuals in one population as 128 and evaluated until 200 generations. The value of mutation and crossover probabilities are set as 0.3. We set the range of search space empirically tabulated in Table. I.

Table I
Range value of the optimized parameter

Definition	Notation	Range value	Optimized value
Activation time of PF's firing (H) for hindlimb and (F) for forelimb	$\phi_1^{(H)}$	-2.0 to 10.0	0.034
	$\phi_2^{(H)}$	-2.0 to 10.0	0.230
	$\phi_1^{(F)}$	-2.0 to 10.0	3.934
	$\phi_2^{(F)}$	-2.0 to 10.0	0.0143
Duration of PF's firing	$\psi_1^{(H)}$	5.0 to 45.0	13.234
	$\psi_2^{(H)}$	5.0 to 45.0	29.756
	$\psi_1^{(F)}$	5.0 to 45.0	1.320
	$\psi_2^{(F)}$	5.0 to 45.0	32.120
Gain parameter for stretch reflex muscle. $G^{l,S}$ represents the gain during swing phase	$G^{l,S}_{BFA}$, $G^{l,S}_{IP}$	200 to 400	238.2
	G^{l}_{BFA}, G^{l}_{IP}	300 to 1100	1080
	G^{l}_{SF}, G^{l}_{SE}	50 to 150	50.2
	G^{l}_{EF}, G^{l}_{EE}	200 to 800	543.8
	G^{l}_{SF}	200 to 600	569.6
Stretch muscle offset	$l_{off,BFA}$	0.0002 to 0.0006	0.000247
	$l_{off,SF}$	-0.0001 to 0.0003	0.000073
	$l_{off,EF}$	0.0005 to 0.0013	0.001085
Gain parameter for force reflex muscle	G^{F}_{BFP}, G^{F}_{VA}	3.5 to 8.5	3.51
	G^{F}_{BFA}, G^{F}_{IP}	0.5 to 3.5	3.455
	G^{F}_{SE}	100 to 300	255.199
	G^{F}_{SF}	3.0 to 7.0	6.952
	$G^{F,A}_{SF}$	1.0 to 5.0	2.02
Constant parameter in muscle stimulation,	C^{sf}_{BFP}	0.65 to 1.35	0.9846
	C_{VA}	0.1 to 1.0	0.161
	C_{BFP}	0.0 to 0.2	0.199
	C_{EE}	0.4 – 0.8	0.73
	C_{WF}	0.2 to 0.4	0.2058
Gain parameters for firing rate signal from PF neurons	G^{Y}_{VA}	0.1 to 1.0	0.836
	G^{Y}_{BFP}	0.1 to 1.0	0.242
	G^{F}_{BFP}	0.1 to 1.0	0.379
	G^{Y}_{SF}, G^{Y}_{SE}	0.0 to 1.0	0.009
	G^{Y}_{EF}, G^{Y}_{EE}	0.0 to 1.0	0.017
	G^{Y}_{EF}, G^{Y}_{EE}	0.0 to 1.0	0.095

We run the robot in simulation after a 1000 time cycle (5 seconds) to evaluate and measure the fitness score. In this evaluation we concentrate on improving parameters of muscle reflex and pattern formation. In CPG structure, RG structure is set similar to the previous model in [18]. The result of Pareto front in a certain generation can be seen in Fig. 4. There are 95 solutions in the Pareto front provided in the final result. However, in order to perform and analyze, we take the most compromise solution that shows in Table. I.

In order to show the effectiveness of the proposed model, we tested the muscle reflex model with three different signal input patterns shown in Figs. 8. The first signal input indicates a walking type gait pattern. The second signal input indicates a slow walking type gait pattern. The third signal input indicated trot type gait pattern. These signal patterns are generated from

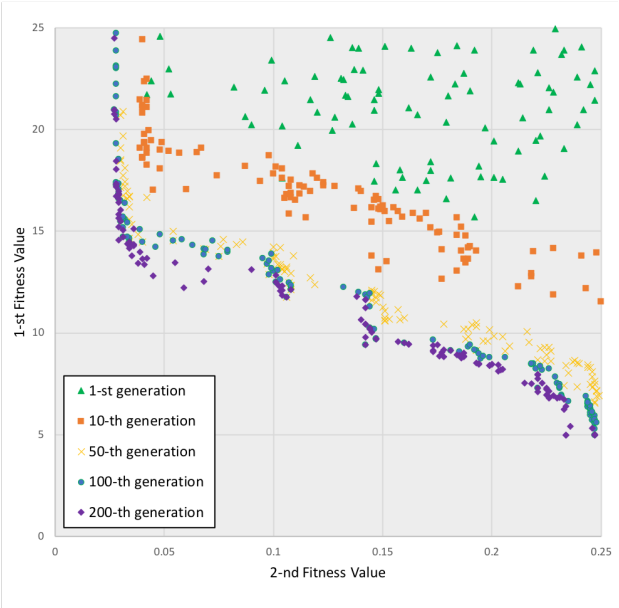

Figure 4. Evolution of pareto front in certain generation. The population moved to the minimum value of the fitness function. The difference between distance traveled and desired distance is decreased, the torso movement oscillation and the total muscle stimulation tend to decrease

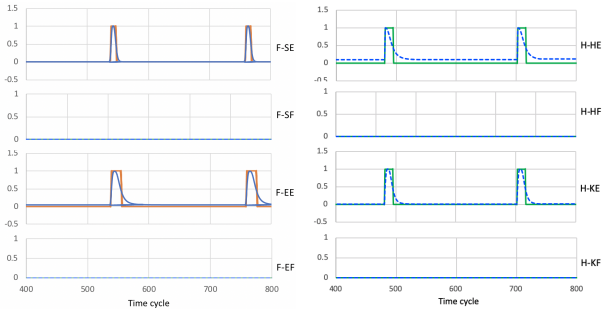

(a) (b)

Figure 5. Input signal from pattern formation neuron in each leg. a) Signal pattern of forelimb b) Signal pattern of hindlimb

our previous work [32].

The result shows the simulated robot was able to move in different input of pattern formation from the CPG level. A sample snapshot of robot performance in simulation can be seen in Fig. 6. The various input signal causes a different muscle activation pattern as well as muscle torque. The recorded torque of the muscles can be seen in Fig. 8.

In order to evaluate the stability of the robot's movement, we analyze the robot's torso acceleration and speed in three different signal inputs. The robot has smooth movement in all given inputs where the acceleration oscillation is lower than 0.05 m/s^2. The faster speed performance is more stable than the other performances.

V. Conclusion

We have developed a muscle-based locomotion model in a Quadruped robot inspired by the Felidae species principle,

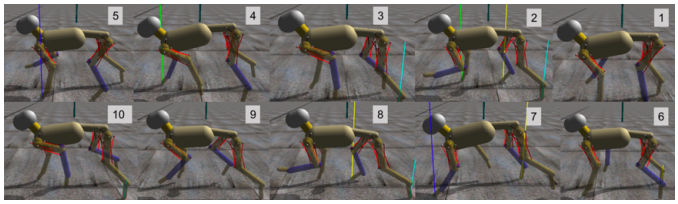

Figure 6. The snapshot of robot's performance in Open Dynamics Engine

composed of pattern and muscle activation control. In this paper, we focus on the development of muscle activation control. We developed a muscle reflex model of forelimb and hindlimb structure in the swing and stance phase. We successfully optimized the muscle reflex parameters using MOEA with 128 individuals in 500 generations. Results showed that the robot's speed and movement pattern can be controlled by regulating simple stimulation signals from pattern formation. Based on the movement evaluation, the proposed muscle-based locomotion performs smooth movements with low moving oscillation. Maximum oscillation value ranges only from -0.05 m/s^2 to 0.05 m/s^2. In addition, the muscle reflex model is able to perform a stable movement with different input of pattern and timing. The role of pattern formation allows each muscle to activate with different timing in the swing phase. The muscle reflex model is ready to be integrated with higher-level controller from CPG as well as MLR. The present contribution does not concentrate on advance implementation, but tends to analyze the scientific problem which may occur when exploring the advantages of Felidae family of animal-like musculoskeletal systems for a quadruped robot.

The locomotion of human or animal is considered not merely rely on the role of muscle reflex integration. In fact, it has a complex mechanism that involves their cognitive with external sensory integration. For future works, we will consider the role of movement-related cognitive information to achieve dynamic locomotion.

References

[1] S. Kajita *et al.*, "Biped walking pattern generation by using preview control of zero-moment point," in *IEEE International Conference on Robotics and Automation*, vol. 2. IEEE, 2003, pp. 1620–1626.

[2] A. A. Saputra, A. S. Khalilullah, I. A. Sulistijono, and N. Kubota, "Adaptive motion pattern generation on balancing of humanoid robot movement," in *28th Canadian Conference on Electrical and Computer Engineering*, 2015, pp. 1479–1484.

[3] A. J. Ijspeert, "Central pattern generators for locomotion control in animals and robots: a review," *Neural networks*, vol. 21, no. 4, pp. 642–653, 2008.

[4] A. A. Saputra, J. Botzheim, I. A. Sulistijono, and N. Kubota, "Biologically inspired control system for 3-d locomotion of a humanoid biped robot," *IEEE Transactions on Systems, Man, and Cybernetics: Systems*, vol. 46, no. 7, pp. 898–911, 2015.

[5] T. Geijtenbeek, M. Van De Panne, and A. F. Van Der Stappen, "Flexible muscle-based locomotion for bipedal creatures," *ACM Transactions on Graphics (TOG)*, vol. 32, no. 6, p. 206, 2013.

[6] T. G. Brown, "On the nature of the fundamental activity of the nervous centres; together with an analysis of the conditioning of rhythmic activity in progression, and a theory of the evolution of function in the nervous system," *The Journal of physiology*, vol. 48, no. 1, pp. 18–46, 1914.

[7] G. N. Orlovskiĭ, T. Deliagina, and S. Grillner, *Neuronal control of locomotion: from mollusc to man*. Oxford University Press, 1999.

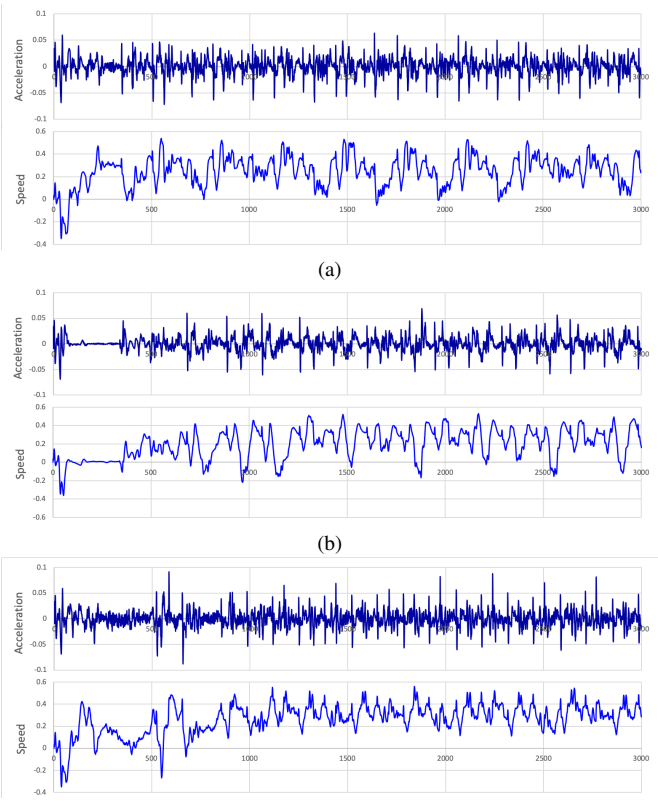

Figure 7. The recorded robot's torso acceleration and speed in different signal pattern input a) normal speed b) slower speed c) faster speed

[8] I. A. Rybak *et al.*, "Modelling spinal circuitry involved in locomotor pattern generation: insights from the effects of afferent stimulation," *The Journal of physiology*, vol. 577, no. 2, pp. 641–658, 2006.

[9] K. Pearson, Ö. Ekeberg, and A. Büschges, "Assessing sensory function in locomotor systems using neuro-mechanical simulations," *Trends in neurosciences*, vol. 29, no. 11, pp. 625–631, 2006.

[10] K. Tsujita, T. Kobayashi, and T. Masuda, "Feasibility study on stability of gait patterns with changeable body stiffness using pneumatic actuators in a quadruped robot," *Advanced robotics*, vol. 23, no. 5, pp. 503–520, 2009.

[11] Y. Yamada, S. Nishikawa, K. Shida, R. Niiyama, and Y. Kuniyoshi, "Neural-body coupling for emergent locomotion: A musculoskeletal quadruped robot with spinobulbar model," in *2011 IEEE/RSJ International Conference on Intelligent Robots and Systems*. IEEE, 2011, pp. 1499–1506.

[12] M. Toeda, S. Aoi, S. Fujiki, T. Funato, K. Tsuchiya, and D. Yanagihara, "Gait generation and its energy efficiency based on rat neuromusculoskeletal model," *Frontiers in Neuroscience*, vol. 13, p. 1337, 2019.

[13] I. A. Rybak *et al.*, "Modelling spinal circuitry involved in locomotor pattern generation: insights from deletions during fictive locomotion," *The Journal of physiology*, vol. 577, no. 2, pp. 617–639, 2006.

[14] K. Pearson, "Role of sensory feedback in the control of stance duration in walking cats," *Brain research reviews*, vol. 57, no. 1, pp. 222–227, 2008.

[15] T. G. Brown, "The intrinsic factors in the act of progression in the mammal," *Proceedings of the Royal Society of London. Series B, containing papers of a biological character*, vol. 84, no. 572, pp. 308–319, 1911.

[16] K. Matsuoka, "Mechanisms of frequency and pattern control in the neural rhythm generators," *Biological Cybernetics*, vol. 56, pp. 345–353, 1987.

[17] ——, "Sustained oscillations generated by mutually inhibiting neurons with adaptation," *Biological Cybernetics*, vol. 52, pp. 367–376, 1985.

[18] A. A. Saputra, N. N. W. Tay, Y. Toda, J. Botzheim, and N. Kubota, "Bézier curve model for efficient bio-inspired locomotion of low cost four legged robot," in *2016 IEEE/RSJ International Conference on Intelligent Robots and Systems (IROS)*. IEEE, 2016, pp. 4443–4448.

[19] A. A. Saputra, I. A. Sulistijono, J. Botzheim, and N. Kubota, "Interconnection structure optimization for neural oscillator based biped robot locomotion," in *IEEE Symposium Series on Computational Intelligence*, 2015, pp. 288–294.

[20] J. R. Hinchliffe and D. R. Johnson, *The development of the vertebrate limb: an approach through experiment, genetics, and evolution*. Oxford University Press, USA, 1980.

[21] D. A. McVea, J. M. Donelan, A. Tachibana, and K. G. Pearson, "A role for hip position in initiating the swing-to-stance transition in walking cats," *Journal of neurophysiology*, vol. 94, no. 5, pp. 3497–3508, 2005.

[22] T. Lam and K. G. Pearson, "Proprioceptive modulation of hip flexor activity during the swing phase of locomotion in decerebrate cats," *Journal of Neurophysiology*, vol. 86, no. 3, pp. 1321–1332, 2001.

[23] A. Spröwitz *et al.*, "Towards dynamic trot gait locomotion: Design, control, and experiments with cheetah-cub, a compliant quadruped robot," *The International Journal of Robotics Research*, vol. 32, no. 8, pp. 932–950, 2013.

[24] H. Witte *et al.*, "Transfer of biological principles into the construction of quadruped walking machines," in *in Proc. of the Second International Workshop on Robot Motion and Control*, 2001, pp. 245–249.

[25] H. Geyer and H. Herr, "A muscle-reflex model that encodes principles of legged mechanics produces human walking dynamics and muscle activities," *IEEE Transactions on neural systems and rehabilitation engineering*, vol. 18, no. 3, pp. 263–273, 2010.

[26] H. Geyer, A. Seyfarth, and R. Blickhan, "Positive force feedback in bouncing gaits?" *Proceedings of the Royal Society of London. Series B: Biological Sciences*, vol. 270, no. 1529, pp. 2173–2183, 2003.

[27] A. W. ENGLISH, "An electromyographic analysis of forelimb muscles during overground stepping in the cat," *Journal of Experimental Biology*, vol. 76, no. 1, pp. 105–122, 1978.

[28] F. Caliebe *et al.*, "Cat distal forelimb joints and locomotion: an x-ray study," *European Journal of Neuroscience*, vol. 3, no. 1, pp. 18–31, 1991.

[29] T. Drew and S. Rossignol, "A kinematic and electromyographic study of cutaneous reflexes evoked from the forelimb of unrestrained walking cats," *Journal of neurophysiology*, vol. 57, no. 4, pp. 1160–1184, 1987.

[30] R. L. Lieber, B. M. Fazeli, and M. J. Botte, "Architecture of selected wrist flexor and extensor muscles," *The Journal of hand surgery*, vol. 15, no. 2, pp. 244–250, 1990.

[31] B. P. Livingston and T. R. Nichols, "Effects of reinnervation of the triceps brachii on joint kinematics and electromyographic patterns of the feline forelimb during level and upslope walking," *Cells Tissues Organs*, vol. 199, no. 5-6, pp. 405–422, 2014.

[32] A. A. Saputra and N. Kubota, "Synthesis of neural oscillator based dynamic rhythmic generation in quadruped robot locomotion," in *2018 International Electronics Symposium on Knowledge Creation and Intelligent Computing (IES-KCIC)*. IEEE, 2018, pp. 184–191.

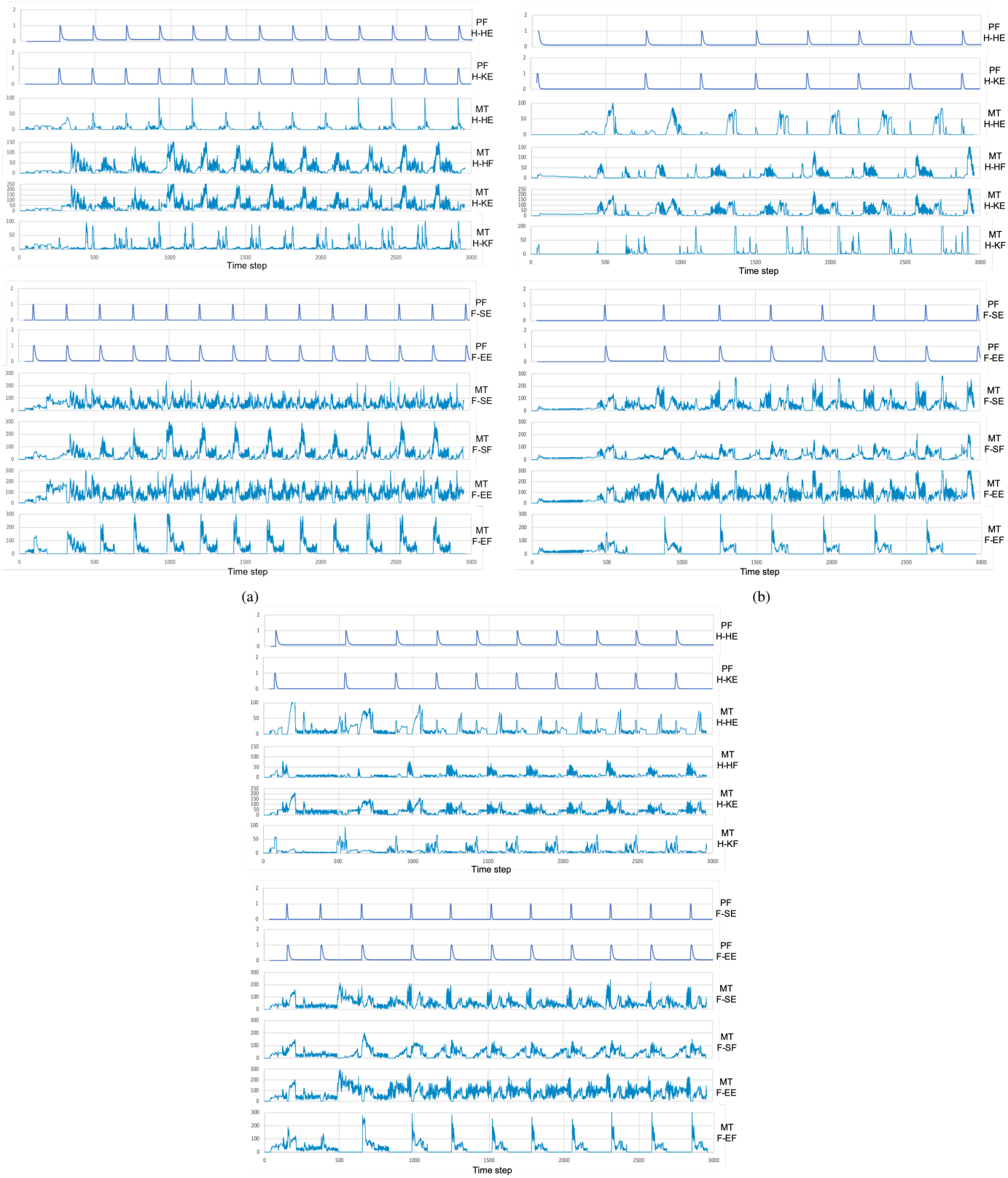

Figure 8. The recorded muscle torque in different moving pattern and speed, input of pattern formation signal to all limb a) slower speed b) normal speed c) faster speed

.